Chemical Physics 170 (1993) 295–301
North-Holland

ac-Driven quantum decay

Frank Grossmann [1] and Peter Hänggi
University of Augsburg, Institute of Physics, Memminger Strasse 6, W-8900 Augsburg, Germany

Received 12 May 1992

We study the enhancement of the quantum decay rate out of a metastable state, via tunneling, in presence of an external sinusoidal force. It is shown that the Floquet picture of quantum mechanics, together with the complex scaling method, provides an adequate methodology to describe the periodically driven decay process in a nonperturbative way. In the limiting cases of extremely slow and fast external forces the numerical results are compared with simple semiclassical estimates. The decay near the fundamental resonance assumes a Lorentzian line shape in agreement with recent experiments on Josephson junctions in the deep quantum regime. For small forces the enhancement grows proportional to the square of the forcing strength and saturates above a threshold value. Additionally our results also exhibit secondary resonances: at higher frequency corresponding roughly to a second harmonic induced by the nonlinear potential shape, and at lower frequency, exactly at the half of the first resonance, revealing a two-photon transition.

1. Introduction

In this work we focus on the problem of the quantum decay out of a metastable state in presence of external periodic driving. In recent years the decay theory of unstable states [1] has been extended to quantum systems interacting with an environment which includes dissipation [2,3]. Our investigations have been motivated by recent experiments on rf-stimulated biased Josephson junctions both in the classical and the quantum regime [4]. Likewise our study should also be of relevance in quantum chemistry, surface physics and quantum biology when considering photon-assisted dissociation reactions (decays) involving "precursor"-induced barriers or energetic angular-momentum obstructions.

In contrast to the classical regime where the effect is generally known as resonance activation [5], there exist no previous theoretical studies which address the deep quantum regime at zero temperature in a nonperturbative manner. Here we present a full account of the decay rate enhancement of the ground state induced by an external sinusoidal force. In doing so we shall cover the whole frequency regime extending from zero frequency to very high frequencies. The two extreme cases can both be tackled on analytical grounds whereas the intermediate regime – except at resonances between the external frequency and internal level spacings – can be treated on numerical grounds only.

In section 2 we will present the theoretical model that will be studied subsequently, pointing out one of its experimental realizations. Section 3 gives a brief review of the Floquet theoretic approach to unstable systems. In the fourth section we treat the undriven ($S=0$), the adiabatic and the high frequency case. Section 5 deals with the near-resonance case when the frequency of the external force approximately equals the spacing between the ground state and higher excited states. In section 6 we summarize our work and discuss possible future applications.

2. Model Hamiltonian

The starting point of our investigations is the driven Hamiltonian of a particle in a cubic metastable landscape,

[1] Present address: Department of Chemistry, BG-10, University of Washington, Seattle, WA, 98195 USA.

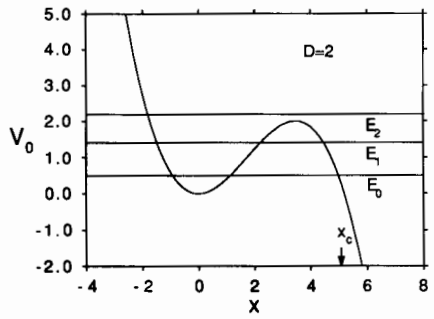

Fig. 1. Unperturbed ($S=0$) metastable potential $V_0(x)$ of the Hamiltonian in eq. (1) with $D=2$, supporting two quasistationary states under the barrier; the horizontal lines indicate the positions of the real parts E_0, E_1, E_2 of the resonance energies; x_c denotes the exit point of the potential.

$$H(x,t) = -\tfrac{1}{2}\partial_x^2 + V_0(x) + xS\sin(\omega t)$$
$$\equiv -\tfrac{1}{2}\partial_x^2 + \tfrac{1}{2}x^2 - \frac{1}{2x_c}x^3 + xS\sin(\omega t)\,. \qquad (1)$$

Here we use dimensionless units. Time is measured in units of $1/\omega_0$, with ω_0 denoting the angular frequency of small oscillations at the bottom of the well. The external frequency ω and energies are thus measured in units of ω_0 and $\hbar\omega_0$. The dimensionless barrier height D is connected to the exit point (the coordinate is measured in units of $\sqrt{\hbar/m\omega_0}$, with m the mass of the particle) of the potential $V_0(x)$ by $x_c=\sqrt{\frac{27}{2}D}$, see fig. 1.

The model in (1) is motivated because the cubic potential approximately describes the decay of the (macroscopic) phase in a current-biased Josephson junction. The frequency of small oscillations is then given by the plasma frequency $\omega_p=\sqrt{(2e/C\hbar)I_c}$ and the dimensionless force strength is $S=I_{ext}/2e\omega_p$. Here C and I_c denote the capacitance and critical current of the junction and I_{ext} is the amplitude of an external sinusoidal microwave current. We will henceforth deal with systems containing only one or two unperturbed resonance states (see below) under the barrier, which corresponds to the experimental setup used for macroscopic quantum tunneling [4].

3. Floquet theory for decaying systems

To obtain a detailed description of the decay process in presence of an external periodic force, we refrain from the use of time-dependent perturbative, semiclassical methods alone. In these approaches [6], the periodicity of the Hamiltonian is not fully exploited. Moreover at strong forcing the perturbative approach no longer suffices. The concept which seems most appropriate for a rigorous treatment is the Floquet picture of quantum mechanics [7]. Given (1), solutions of the time-dependent Schrödinger can be cast in the form

$$\Psi_\epsilon(x,t) = \Phi_\epsilon(x,t)\exp(-i\epsilon t)\,, \qquad (2)$$

$$\Phi_\epsilon(x,t) = \Phi_\epsilon(x,t+T)\,, \qquad (3)$$

where the Floquet function $\Phi_\epsilon(x,t)$ is periodic with the period $T=2\pi/\omega$ of the external force and the quasienergies ϵ determine the long-time behaviour of the wavefunction.

Generally the decay of unstable states can be associated with complex-valued poles of the S-matrix. These correspond to simple poles on the unphysical sheet of the complex-valued energy Riemann surface and constitute the well-known resonance states. By use of the complex-scaling approach [8], i.e. if one rotates the coordinate $x\to xe^{i\phi}$, one uncovers the resonance poles in the complex plane and ends up with square integrable eigenfunctions [9], denoted by $|\phi_n\rangle = |n\rangle$ in the undriven case.

Here we apply this concept generalized to the quasienergy approach. The decay rate Γ in the periodically driven case is then given by the imaginary part of the Floquet resonances (complex-valued quasienergies) as

$$\Gamma_\epsilon = -2\,\mathrm{Im}\,\epsilon\,. \qquad (4)$$

Because we treat the zero temperature limit, we confine ourselves to the rate enhancement γ_0 of the lowest unperturbed resonance state, i.e.

$$\gamma_0 = \frac{\Gamma_{\epsilon_0}-\Gamma_0}{\Gamma_0}\,, \qquad (5)$$

where ϵ_0 denotes the "lowest quasienergy". Note that the quasienergies can be defined only modulo ω, i.e. $\epsilon_{0,k}\equiv\epsilon_0+k\omega$; $k=0,\ \pm1,\ \pm2,\ \ldots$. The quasienergy ϵ_0 merges into the lowest resonance E_0 with imaginary part $\Gamma_0=-2\,\mathrm{Im}\,E_0$, as the amplitude S of the external force approaches zero.

4. Limiting cases

Before we focus on the most interesting regime of resonant driving, $\omega \approx 1$, we first deal with the undriven ($S=0$) and the two limiting cases of adiabatic ($\omega \ll \Gamma_0$) and very fast ($\omega \gg 1$) driving.

4.1. Undriven case

In the undriven ($S=0$) case we have calculated the decay rates out of the resonance states (compare fig. 1 for the case $D=2$) as a function of the barrier height. In table 1 we present the rates for the three lowest states at three different values of D. The decay rates Γ_i monotonically decrease with increasing D; for fixed D they increase with increasing index i.

4.2. Adiabatic case

Following the mathematical reasoning put forward recently for an adiabatically driven symmetric double-well configuration [10], we obtain with an average over the slowly varying phase the "adiabatic rate enhancement" as

$$\Gamma_{\epsilon_0}^{\mathrm{ad}} = \Gamma_0 \frac{1}{2\pi} \int_0^{2\pi} \left(1+6\frac{S\sin(\phi)}{x_c}\right)^{3/4} \times \exp\left\{-\tfrac{36}{5} D\left[\left(1+6\frac{S\sin(\phi)}{x_c}\right)^{3/2} - 1\right]\right\} \mathrm{d}\phi. \quad (6)$$

In fig. 2a we compare the semiclassical approximation (6) (solid line) with the numerical exact results (circles). The excellent agreement for the absolute rate is due to the fact that we used for Γ_0 in (6) the numerical value and not its semiclassical estimate (which exceeds the numerical result by 36% for the parameters we used [9]). The shape of the enhancement, being proportional to S^2 for weak fields, is thus well described by its semiclassical estimate!

Table 1
Numerical values of the undriven ($S=0$) decay rates out of the resonance states of the cubic metastable potential (eq. (1)) as a function of the barrier height D

D	Γ_0	Γ_1	Γ_2
1	4.5400×10^{-3}	2.2686×10^{-1}	1.0103
2	5.8308×10^{-6}	2.7220×10^{-3}	1.3854×10^{-1}
3	5.56×10^{-9}	5.183×10^{-6}	1.5403×10^{-3}

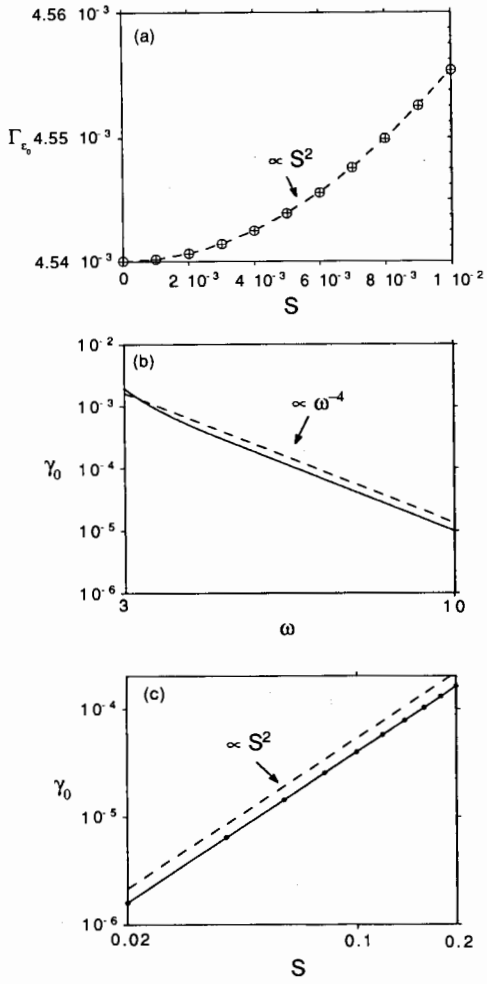

Fig. 2. (a) Adiabatic dimensionless decay rate Γ_{ϵ_0} of the driven metastable potential for the parameters $D=1$, $\omega=10^{-3}$; dashed line: semiclassical result, circles: numerical result. (b, c) Double logarithmic plot of the high-frequency rate enhancement γ_0 of the driven decay problem for the parameters: (b) $D=1$, $S=2\times10^{-1}$; (c) $D=1$, $\omega=5$. Full line: numerical result, dashed line: semiclassical result.

4.3. High-frequency case

In the other extreme limit of very high frequencies, the decay rate can be obtained again within semiclassical accuracy by use of two Kramers–Henneberger transformations (see ref. [10]) and a final cycle averaging. In this way one finds the approximate result

$$\Gamma_{\epsilon_0}^{\mathrm{HF}} \approx \Gamma_0 \left[1 + \left(\frac{36}{10} - \frac{1}{4D} \right) \frac{S^2}{\omega^4} \right], \quad \omega \gg 1 . \tag{7}$$

In figs. 2b and 2c we depict the rate enhancement defined in eq. (5). The semiclassical result (dashed lines) is compared with the numerical precise values (solid lines) as a function of ω (fig. 2b) and S (fig. 2c), respectively. The power-law behaviour predicted in (7) is thereby confirmed by the numerics. Note that for $\omega \to \infty$, the high-frequency limit approaches the unperturbed (zero frequency) value proportional to ω^{-4}. Clearly, as $\omega \to \infty$ the system is no longer capable to respond to the external perturbation and therefore the extreme fast limit reduces to the extreme adiabatic limit, i.e. $\Gamma_{\epsilon_0} = \Gamma_0$.

5. Near resonance

Let us now consider the most interesting regime of frequencies near resonance $\omega \approx \omega_1 \equiv \mathrm{Re}(E_1 - E_0) \overset{D=2}{\approx} 0.9057$ (see fig. 1). For the numerical investigations we used a barrier height of $D = 2$.

5.1. Below threshold

First we have looked at the rate enhancement for values of the external force strength *lower* than a certain threshold value S_t, which will be determined in subsection 5.3. For external dimensionless forces of $S = 7 \times 10^{-4}$ (broken line in fig. 3a) and $S = 1.5 \times 10^{-3}$ (solid line in fig. 3a) the numerical values for the enhancement γ_0 of the decay rate are depicted versus the external driving frequency. At the resonance frequency $\omega = \omega_1$ we find a dramatic increase in the rate enhancement from $\gamma_0(\omega_1,\ S = 7 \times 10^{-4}) \approx 17$ to $\gamma_0(\omega_1, S = 1.5 \times 10^{-3}) \approx 94$ by tuning up the external forcing. This drastic increase is well approximated by the result in eq. (20) derived below!

The line shape of the enhancement curves is rather symmetric around the resonance frequency. This driven tunneling-induced Lorentzian-like rate enhancement is in clear contrast to the very asymmetric energy-diffusion induced enhancement found in classical resonance activation [5]. On theoretical grounds this symmetric shape is due to the frequency

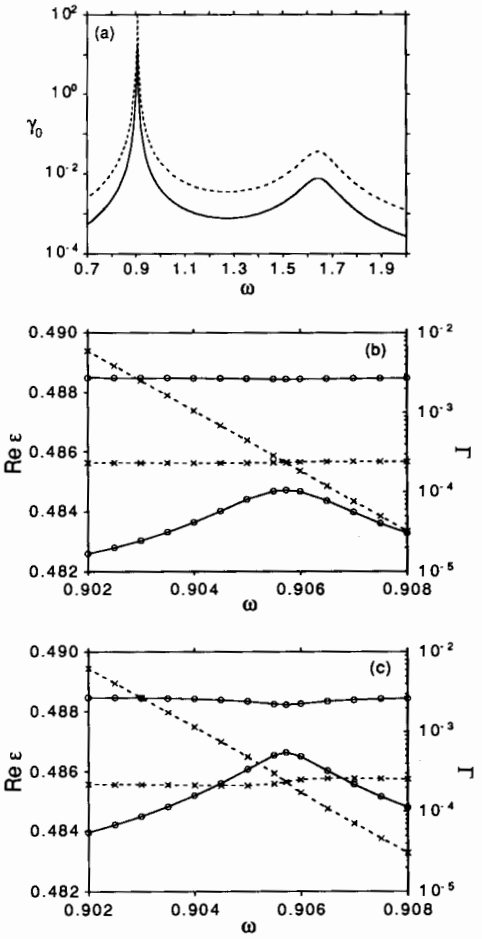

Fig. 3. (a) Numerical values for the rate enhancement of the lowest resonance state γ_0 as a function of frequency for the driven decay problem. The parameters are $D = 2$, $S = 7 \times 10^{-4}$ (solid line), $D = 2$, $S = 1.5 \times 10^{-3}$ (broken line). (b, c) Behaviour of the real parts (crosses) and imaginary parts (circles) of the quasienergies ϵ_0, $\epsilon_1 - \omega$ near the first resonance frequency for $S = 7 \times 10^{-4}$ (b) and $S = 1.5 \times 10^{-3}$ (c) (the axis for the imaginary parts has a logarithmic scale).

behaviour of the real and imaginary parts of the corresponding complex-valued quasienergies (see figs. 3b and 3c). At resonance the corresponding real parts $\mathrm{Re}\,\epsilon_0$, $\mathrm{Re}\,\epsilon_1 - \omega$ of the quasienergies exhibit an *exact crossing*, while the imaginary parts *avoid to cross* each other; both processes occur symmetrically around $\omega = \omega_1$.

Additionally we find a second-harmonic-like transition near $\omega \approx \omega_2 \equiv \mathrm{Re}(E_2 - E_0) \approx 1.6459$ (see fig. 3a). While within a harmonic approximation of the

well this second transition is forbidden, the anharmonicity of the cubic potential gives rise to a non-vanishing dipole matrix element $\langle 0|x|2\rangle$ which characterizes the strength of this higher-order transition. The width of this second resonance for $S=7\times10^{-4}$ is enhanced by a factor $\alpha\approx\Gamma_2/\Gamma_1\approx51$, see table 1. This is due to the fact that the widths of the higher levels making up the resonances obey $\Gamma_2>\Gamma_1>\Gamma_0$. This result can also be deduced in a two-level approximation by a perturbation-type expansion of eq. (7) in ref. [11] for low values of S. The two widths $\delta_{1,2}$ at half maximum of the two peaks of γ_0 at $\omega\approx\omega_1$ and $\omega\approx\omega_2$, respectively, are approximated by $\delta_{1,2}\approx\Gamma_{1,2}-\Gamma_0\approx_{D=2}\Gamma_{1,2}$.

5.2. Above threshold

For external forces *larger* than the threshold value S_t, the height of the enhancement curve at the first resonance ($\omega\approx\omega_1$) is nearly independent of S. This fact can be observed in fig. 4a where $\gamma_0(\omega\approx\omega_1, S=5\times10^{-3})\approx237$ and $\gamma_0(\omega\approx\omega_1, S=1\times10^{-2})\approx245$.

As depicted in figs. 4b and 4c the real parts Re ϵ_0, Re $\epsilon_1-\omega$ of the quasienergies exhibit – in clear contrast to the case with driving strengths $S<S_t$ – an *avoided crossing* at resonance, while the imaginary parts *cross* each other. We note that the main resonance undergoes a shift of its central frequency proportional to the square of the applied external amplitude. This feature is analogous to the Bloch–Siegert shift in magnetic resonance described by a sinusoidally driven two-level quantum dynamics [12]. The shift is depicted in fig. 4c and amounts approximately $\delta\omega_1\approx2\times10^{-4}$.

We also found a small peak located at precisely the half of the first resonance frequency $\omega=\frac{1}{2}\omega_1\approx0.453$ (see fig. 4a). Clearly this subharmonic transition can be viewed as a two-photon stimulated decay process. The peak height $\gamma_0(\frac{1}{2}\omega_1)$ grows proportional with S^l with l exceeding the value $l=2$ expected for single-photon transitions at small fields. The peak at $\omega=\frac{1}{2}\omega_1$ has only been observed for strong driving $S>S_t$ (see subsection 5.3).

At the end of this section, we want to emphasize that the particle decays out of the Floquet state with quasienergy ϵ_0. Far away from one of the resonances, this state has the same structure as the lowest unperturbed wavefunction, which is approximately a Gaussian wave packet centered around the minimum of the well. Near the avoided crossing, however, the Floquet state has also admixtures from the first excited resonance wavefunction [13].

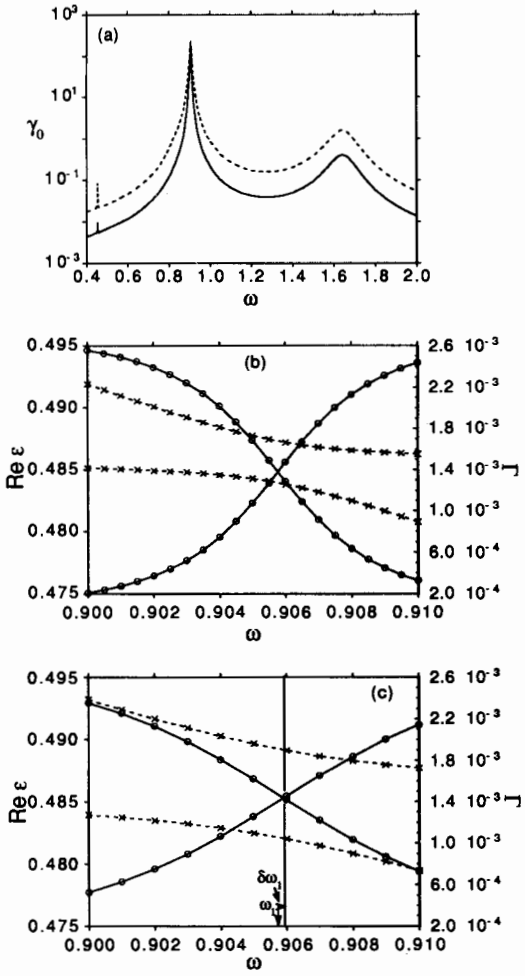

Fig. 4. (a) Numerical values for the rate enhancement of the lowest resonance state γ_0 as a function of frequency for the driven decay problem with the parameters $D=2$, $S=5\times10^{-3}$ (solid line), $D=2$, $S=10^{-2}$ (broken line). (b, c) Behaviour of the real parts (crosses) and imaginary parts (circles) of the quasienergies ϵ_0, $\epsilon_1-\omega$ near the first resonance frequency for $S=5\times10^{-3}$ (b) and $S=10^{-2}$ (c). The Bloch–Siegert shift $\delta\omega_1$ is depicted in (c).

5.3. Two-level treatment at resonance

In this section we will sketch a simple derivation of the threshold value S_t above which the maximal rate enhancement saturates. To this end we employ a driven two-level approximation of the decay problem that will be solved analytically in a rotating wave approximation at resonance.

Treating the cubic term in the potential (1) as a small perturbation we arrive at the Schrödinger equation for the amplitudes $a_{0,1,2} \equiv \langle 0, 1, 2 | \Psi(t) \rangle$,

$$\mathrm{i}\dot{a}_0(t) = E_0 a_0 + x_i S \sin(\omega t)\, a_i(t)\,, \tag{8}$$

$$\mathrm{i}\dot{a}_i(t) = E_i a_i + x_i S \sin(\omega t)\, a_0(t)\,, \tag{9}$$

where $i=1,2$ and the energies E_i are complex valued and the matrix elements x_i are in leading order given by

$$x_1 = \frac{\langle 0|x|1\rangle}{\langle 0|0\rangle} = \frac{\langle 0|x|1\rangle}{\langle 1|1\rangle} = \frac{1}{\sqrt{2}}, \tag{10}$$

$$x_2 = \frac{\langle 0|x|2\rangle}{\langle 0|0\rangle} = \frac{\langle 0|x|2\rangle}{\langle 2|2\rangle} = \frac{1}{2\sqrt{2}\, x_c}. \tag{11}$$

The system of differential equations (8), (9) can be solved at resonance $\omega_i = \mathrm{Re}(E_i - E_0)$ [14]. After inserting the ansatz

$$a_0(t) = \exp\left[-\mathrm{i}\left(\mathrm{Re}\, E_0 - \mathrm{i}\frac{\Gamma_0+\Gamma_i}{4}\right)t\right] b_0(t)\,, \tag{12}$$

$$a_i(t) = \exp\left[-\mathrm{i}\left(\mathrm{Re}\, E_i - \mathrm{i}\frac{\Gamma_i+\Gamma_0}{4}\right)t\right] b_i(t)\,, \tag{13}$$

and performing a rotating wave approximation we arrive at the system

$$\dot{b}_0(t) = \frac{\Gamma_i - \Gamma_0}{4} b_0(t) - x_i \frac{S}{2} b_i(t)\,, \tag{14}$$

$$\dot{b}_i(t) = \frac{\Gamma_0 - \Gamma_i}{4} b_i(t) + x_i \frac{S}{2} b_0(t)\,, \tag{15}$$

The eigenvalues of its characteristic equation

$$\lambda_\pm = \pm\sqrt{\left(\frac{\Gamma_i-\Gamma_0}{4}\right)^2 - \left(\frac{x_i S}{2}\right)^2} \tag{16}$$

may be (i) real, (ii) equal to zero, or (iii) purely imaginary.

We next compare our two-level calculations with the results of the Floquet-theoretical approach. To this end we consider the time evolution of the quantity

$$|a_0(t)|^2 + |a_i(t)|^2 \tag{17}$$

with the initial conditions

$$a_0(0) = 1\,, \quad a_i(0) = 0\,. \tag{18}$$

In the case of real eigenvalues, the sum of the squares (17) will exhibit *three* exponentially decaying terms. The smallest of these rates

$$\Gamma_0^{\mathrm{tl}}(\omega_i) = \frac{\Gamma_i+\Gamma_0}{2} - \sqrt{\left(\frac{\Gamma_i-\Gamma_0}{2}\right)^2 - (Sx_i)^2} \tag{19}$$

corresponds to $\Gamma_{\epsilon 0}$. For the rate enhancement at resonance $\omega = \omega_i$ we therefore obtain within the two-level approximation in terms of $R_i \equiv \Gamma_i/\Gamma_0 > 1$

$$\gamma_0(\omega=\omega_i) \approx \gamma^{\mathrm{tl}}(\omega_i) = \tfrac{1}{2}(R_i - 1) - \sqrt{\left(\frac{R_i-1}{2}\right)^2 - \left(\frac{Sx_i}{\Gamma_0}\right)^2}\,. \tag{20}$$

The numerical values for γ_0 at $\omega \approx \omega_1$ given in subsection 5.1 are well approximated by the result in (20).

For zero or purely imaginary eigenvalues, (17) exhibits *only one* exponential with a rate $\Gamma_0^{\mathrm{tl}}(\omega_i)$ given by the mean $\frac{1}{2}(\Gamma_i+\Gamma_0)$ of the two undriven decay rates, being independent of S. Therefore the vanishing of the eigenvalues ($\lambda_\pm = 0$) serves as an estimate for the threshold value

$$S_t = \frac{\Gamma_i - \Gamma_0}{2x_i} \tag{21}$$

above which the rate enhancement saturates. Inserting the numerical values from table 1 for the case $D=2$ we find $S_t \approx 1.92 \times 10^{-3}$ at the first resonance, $\omega \approx \omega_1$. This value just lies between the parameter values used in figs. 3 and 4.

6. Summary

At present time there exist no experimental data which allow for a detailed quantitative comparison with our results. The only existing data are at low but finite temperatures $T > 0$, and in addition the strength of the amplitude (respectively the power) of the external force has not been measured explicitly. Nevertheless, the existing data in ref. [4] (see figs. 18 and 20 therein) typically exhibit the change of shape of

the enhancement curve from a *very asymmetric* shape, with more weight located below the resonance frequency ω_1, characteristic for the classical diffusive regime, towards the *tunneling-induced symmetric* shape at temperatures $T<30$ mK below the crossover temperature to quantum controlled decay. Additionally, the existing data are taken at a force strength (the height of the dimensionless maximum in the resonance curves in ref. [4] is smaller than 2.718...) that is too low to quantitatively locate a Bloch–Siegert shift. Moreover the regime of $\omega\approx\omega_2$ and $\omega\approx\frac{1}{2}\omega_1$ has presently not been covered in the extreme quantum limit by the existing experimental data.

We hope that our new predictions will motivate and guide future experimental efforts, both in the field of macroscopic quantum tunneling phenomena, as well as for photon-assisted tunneling-reactions occurring in the vast field of quantum chemistry.

In conclusion, in this paper we have addressed the rate enhancement induced by an external periodic force in the deep nonsemiclassical quantum regime, and/or for force strengths that are too high for perturbative approaches to be valid. By use of the quasienergy methodology one finds a drastic enhancement around the main first resonance with a characteristic symmetrically peaked lineshape. This enhancement is analytically well described by the formula given in (20). Above a threshold value S_t of the force a saturation of the rate enhancement is observed which could be explained within a two-level approximation. In addition we predict the existence of a resonance shift with increasing amplitude and characteristic additional enhancements of the driven decay rate at the first superharmonic $\omega=\omega_2$, and at the first subharmonic $\omega=\frac{1}{2}\omega_1$. Away from these characteristic regimes the decay rate still is enhanced at all frequencies and can be described analytically via eqs. (6) and (7) in the asymptotic regimes of low and high frequencies.

Acknowledgement

We want to acknowledge financial support by the Deutsche Forschungsgemeinschaft through Grant No. Ha 1517/3-2.

References

[1] L. Fonda, G.C. Ghirardi and A. Rimini, Rept. Progr. Phys. 41 (1978) 587.
[2] A.O. Caldeira and A.J. Leggett, Ann. Phys. (NY) 149 (1983) 374; 153 (1984) 455(E).
[3] P. Hänggi, P. Talkner and M. Borkovec, Rev. Mod. Phys. 62 (1990) 251, see section IX;
P. Hänggi, in: Noise and chaos in nonlinear dynamical systems, Dissipative Quantum Tunneling at Finite Temperatures, eds. F. Moss, L.A. Lugiato and W. Schleich (Cambridge Univ. Press, Cambridge, 1990) pp. 187–206.
[4] J.M. Martinis, M.H. Devoret and J. Clarke, Phys. Rev. B 35 (1987) 4682.
[5] M.H. Devoret, J.M. Martinis, D. Esteve and J. Clarke, Phys. Rev. Letters 53 (1984) 1260; Phys. Rev. B 36 (1987) 58;
B. Carmeli and A. Nitzan, Phys. Rev. A 32 (1985) 2434;
S. Linkwitz and H. Grabert, Phys. Rev. B 44 (1991) 11901.
[6] B.I. Ivlev and V.I. Melnikov, Phys. Rev. Letters 55 (1985) 1614;
A.I. Larkin and Yu.N. Ovchinnikov, J. Low Temp. Phys. 63 (1986) 317;
M.P.A. Fisher, Phys. Rev. B 37 (1988) 75;
K.S. Chow, D. Browne and V. Ambegaokar, Phys. Rev. B 37 (1988) 1624.
[7] J.H. Shirley, Phys. Rev. 138 (1965) B979;
Ya.B. Zeldovich, Sov. Phys. JETP 24 (1967) 1006;
N.L. Manakov, V.D. Ovsiannikov, L.P. Rapoport, Phys. Rept. 141 (1986) 319;
S.-I. Chu, Advan. Chem. Phys. 73 (1986) 739.
[8] Y.K. Ho, Phys. Rept. 99 (1983) 1.
[9] W. Hontscha, P. Hänggi and E. Pollak, Phys. Rev. B 41 (1990) 2210.
[10] F. Grossmann, P. Jung, T. Dittrich and P. Hänggi, Z. Phys. B 84 (1991) 315.
[11] D. Sokolovski, Phys. Letters A 132 (1988) 381.
[12] F. Bloch and A. Siegert, Phys. Rev. 57 (1940) 522.
[13] T. Dittrich and U. Smilansky, Nonlinearity 4 (1991) 59.
[14] F. Grossmann, Ph.D. Thesis, University of Augsburg, Germany (1992).